nature plants

LETTERS

PUBLISHED: 10 APRIL 2017 | VOLUME: 3 | ARTICLE NUMBER: 17043

GW5 acts in the brassinosteroid signalling pathway to regulate grain width and weight in rice

Jiafan Liu[1†], Jun Chen[1†], Xiaoming Zheng[1], Fuqing Wu[1], Qibing Lin[1], Yueqin Heng[1], Peng Tian[1], ZhiJun Cheng[1], Xiaowen Yu[2], Kunneng Zhou[2], Xin Zhang[1], Xiuping Guo[1], Jiulin Wang[1], Haiyang Wang[1]* and Jianmin Wan[1,2]*

Grain size is a major determinant of grain yield in cereal crops. *qSW5/GW5*, which exerts the greatest effect on rice grain width and weight, was fine-mapped to a 2,263-bp/21-kb genomic region containing a 1,212-bp deletion, respectively. Here, we show that a gene encoding a calmodulin binding protein, located ~5 kb downstream of the 1,212-bp deletion, corresponds to *qSW5/GW5*. *GW5* is expressed in various rice organs, with highest expression level detected in young panicles. We provide evidence that the 1,212-bp deletion affects grain width most likely through influencing the expression levels of *GW5*. GW5 protein is localized to the plasma membrane and can physically interact with and repress the kinase activity of rice GSK2 (glycogen synthase kinase 2), a homologue of *Arabidopsis* BIN2 (BRASSINOSTEROID INSENSITIVE2) kinase, resulting in accumulation of unphosphorylated OsBZR1 (*Oryza sativa* BRASSINAZOLE RESISTANT1) and DLT (DWARF AND LOW-TILLERING) proteins in the nucleus to mediate brassinosteroid (BR)-responsive gene expression and growth responses (including grain width and weight). Our results suggest that *GW5* is a novel positive regulator of BR signalling and a viable target for genetic manipulation to improve grain yield in rice and perhaps in other cereal crops as well.

Grain size and shape, specified by its three dimensions (length, width and thickness), have been under extensive selection during rice breeding for their impact on grain yield and appearance quality[1]. Recent studies have shown that rice grain size is controlled by multiple signalling pathways, including the ubiquitination-mediated proteasomal degradation pathway, phytohormones (cytokinin, BR and auxin) and G-protein signalling pathways[2–4]. However, the functional relationships and interactions among these pathways remain largely unknown.

Previous studies reported that *qSW5/GW5* exerts the greatest effect on grain width and weight and was fine-mapped to a 2,263-bp/21-kb genomic region, respectively[5,6]. Strikingly, two distinct open reading frames (ORFs) (ORF1-S and ORF2-W) in this region were proposed to code for *qSW5* (QTL for seed width on chromosome 5) and *GW5* (QTL for grain width and weight on chromosome 5), respectively[5,6] (Supplementary Fig. 1). However, functional complementation tests using these individual ORFs were lacking. In addition, we noted that the predicted ORF2-W in IR24 is terminated prematurely in Kasalath (both IR24 and Kasalath are of slender grain phenotype) (Supplementary Figs 2 and 3). Furthermore, we failed to detect the transcript of ORF1-S/ORF2-W by polymerase chain reaction with reverse transcription (RT–PCR) either in young panicles of Kasalath or IR24 plants, despite repeated attempts (Supplementary Fig. 4). These observations raised the possibility that the identity of *qSW5/GW5* may still remain as an open question.

Our bioinformatic analysis confirmed the three predicted ORFs (ORF1, ORF2 and ORF3) in the 11.2-kb region of Kasalath[6] (http://softberry.com) (Fig. 1a). Transgenic assay with three Kasalath fragments (*J15*, *J17* and *J20*) showed that transformants of *J17* (covering ORF3) and *J20* (covering all three ORFs) exhibited a slender grain phenotype in Nipponbare background, whereas transformants of the *J15* fragment (covering only ORF1 and ORF2) still had wide grains (Fig. 1a–e,h). Consistent with this, a significant decrease in grain width and weight was only observed in the ORF3 overexpressors (*OX3*) (driven by the maize ubiquitin promoter), but not in the ORF1 and ORF2 overexpressors (*OX1* and *OX2*, respectively) (Fig. 1a–h). These results suggest that ORF3 (LOC_Os05g09520) may correspond to *qSW5/GW5*. ORF3 contains two IQ calmodulin-binding motifs and one unknown function domain (DUF4005) (Supplementary Fig. 5). To further verify that ORF3 corresponds to *qSW5/GW5*, we overexpressed ORF3 with mutated IQ motifs (ORF3m); no obvious effects were observed in the ORF3m transgenic plants (*OX3m*) compared with Nipponbare (Fig. 1b–e,h). Conversely, knocking out ORF3 in Kasalath via CRISPR–Cas resulted in significantly increased grain width and weight (Fig. 1b–e and Supplementary Fig. 6). These collective data suggest that ORF3 corresponds to *qSW5/GW5* (we refer to ORF3 as *GW5* hereafter).

Scanning electron microscopy observation showed that *GW5*-overexpressing plants (*OX3*) had fewer epidermal cells in the spikelet hull surface than Nipponbare (Supplementary Fig. 7a,b). Observations of cross-sections of the central part of the spikelet hull showed that the outer parenchyma cell layer in *OX3* was shorter and contained fewer cells than Nipponbare in both outer and inner glumes, but there were no significant differences in cell length (Supplementary Fig. 7c–i), thus verifying the notion that *GW5* regulates spikelet development via controlling cell number of the glume of the rice flower. RT–PCR analysis and rapid amplification of complementary DNA ends (RACE) assay confirmed the expression of *GW5* (Supplementary Fig. 8). Quantitative RT–PCR (RT–qPCR) and *pGW5::GUS* reporter gene analyses revealed that *GW5* was preferentially expressed in developing panicles and the highest levels of *GW5* expression were found in young panicles of ~4 cm in length, whereas less transcript was detected in the root, culm, leaf sheath and mature panicle (>15 cm in length) (Fig. 2a and Supplementary Fig. 9).

Transmembrane prediction using hidden Markov models analysis showed that there is a putative transmembrane region in the amino-terminal region (aa (amino acid): 73–94) of the predicted GW5 protein. To determine the cellular localization of GW5 protein, we

[1]National Key Facility for Crop Gene Resources and Genetic Improvement, Institute of Crop Science, Chinese Academy of Agricultural Sciences, Beijing 100081, China. [2]National key Laboratory for Crop Genetics and Germplasm Enhancement, Jiangsu Plant Gene Engineering Research Center, Nanjing Agricultural University, Nanjing 210095, China. †These authors contributed equally to this work. *e-mail: wanjianmin@caas.cn; wanghaiyang@caas.cn

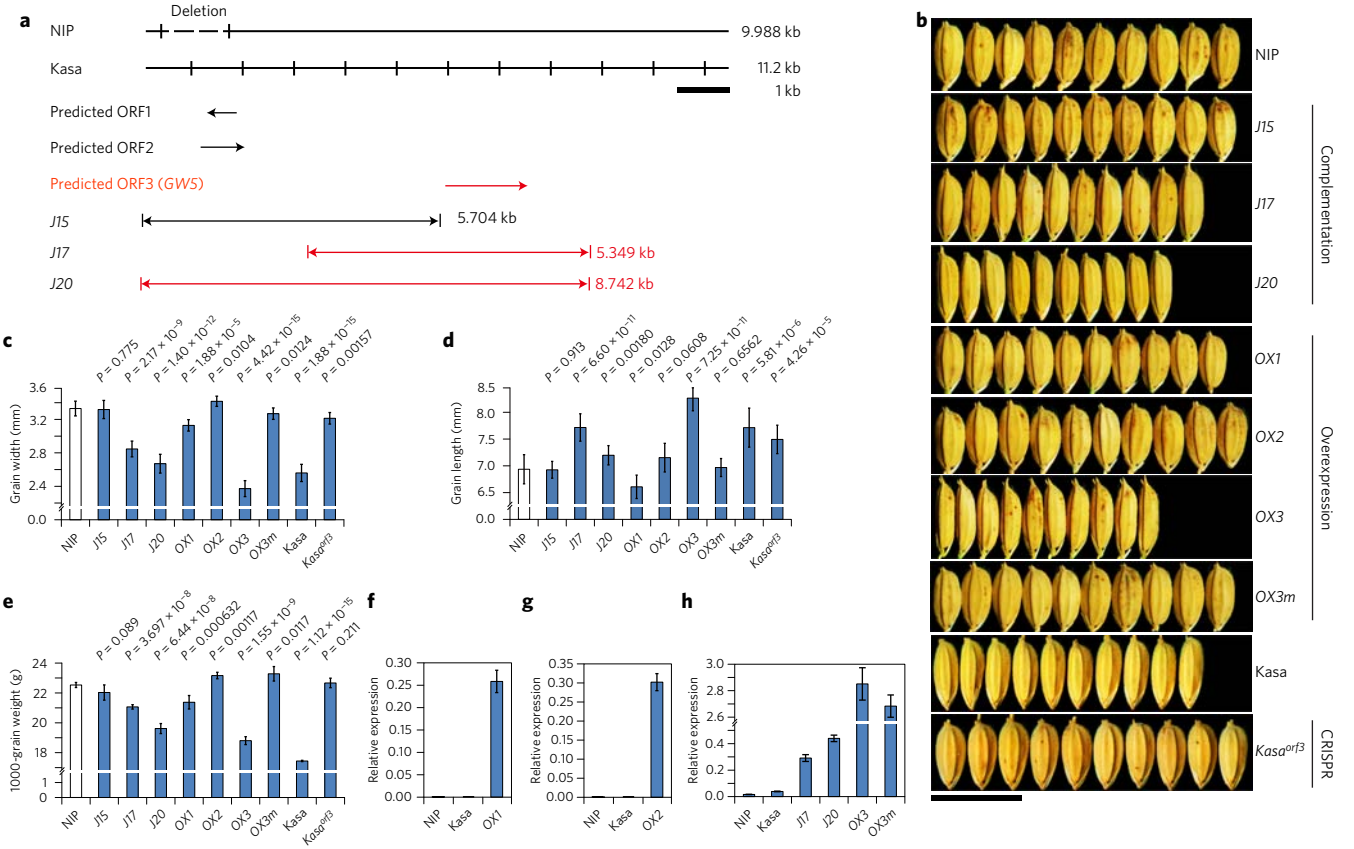

Figure 1 | Identification of *GW5* gene. a, Schematic representation of the genomic structure of Nipponbare (NIP) and Kasalath (Kasa). Positions of the 1,212-bp deletion, the three predicted ORFs and three Kasalath genome fragments used for the complementation test are indicated. **b**, Grains of Nipponbare, Kasalath and the transgenic plants (T1). Scale bar, 10 mm. *OX1, OX2, OX3* and *OX3m* indicate grains from T1 plants overexpressing ORF1, ORF2, ORF3 and ORF3m, respectively. *Kasa*^{orf3} indicates grains from T1 plants knocking out ORF3 in Kasalath via CRISPR-Cas. **c**, Comparison of the grain width among Nipponbare, Kasalath and the transgenic plants ($n = 30$). **d**, Comparison of the grain length among Nipponbare, Kasalath and the transgenic plants ($n = 30$). **e**, Comparison of 1000-grain weight among Nipponbare, Kasalath and the transgenic plants ($n = 5$). *P* values from the student's *t*-test of the transgenic plants against Nipponbare were indicated. **f**–**h**, RT-qPCR analysis of the transcript levels of ORF1 (**f**), ORF2 (**g**) and ORF3/ORF3m (**h**) in young panicles (0.2–2 cm in length for ORF1 and ORF2, ~5 cm in length for ORF3/ORF3m) of various plants. For **f**,**g**: $n = 3$. The values in **c**–**h** represent the mean ± s.d.

fused the full-length cDNA of *GW5* to the N terminus of GFP and transformed it into rice protoplasts. The GW5-GFP fusion protein was exclusively co-localized with the plasma membrane marker (SCAMP1-RFP)[7]. Similarly, GW5-GFP fusion protein was also exclusively localized to the plasma membrane in onion epidermal cells, tobacco leaf epidermal cells and root cells of transgenic rice plants (Supplementary Fig. 10). These results suggest that GW5 protein is localized to the plasma membrane. Phylogenetic analysis revealed that homologues of GW5 could be found in both monocots and eudicots, suggesting that it represents an evolutionarily conserved gene. However, these homologues were clustered into distinct monocot- and dicot-specific groups, with much higher amino acid sequence identities (up to 72%) between GW5 and its monocot homologues (Supplementary Figs 11 and 12).

Comparison of the amino acid sequences of GW5 in Nipponbare and Kasalath revealed an amino acid deletion in Kasalath (Supplementary Fig. 13). To test whether this amino acid deletion is associated with the decreased grain width, we transformed the Kasalath and Nipponbare *GW5* cDNAs driven by the Kasalath *GW5* promoter fused with CaMV 35S enhancer region[8,9] into Nipponbare, respectively. Surprisingly, overexpression of both cDNAs rendered a slender grain phenotype in Nipponbare (Supplementary Fig. 14). As we noted that the level of *GW5* messenger RNA transcript in Nipponbare plants was significantly lower than that in Kasalath plants (Fig. 2a), we thus suspected that differential expression levels of *GW5* in Nipponbare and Kasalath may underlie its effect on grain width. To substantiate this, we compared *GW5* expression levels in different T1 transgenic lines of *K-OX*. Significant negative correlation between grain width and the expression level of *GW5* was observed (Fig. 2b). These results suggest that the expression level of *GW5*, but not the change in its coding sequence, regulates grain width. Consistent with this notion, compared to Nipponbare and Asominori, *GW5* expression level was higher in their near isogenic lines ZP140 and CSSL28, respectively (Fig. 2c).

Previously, Shomura *et al.*[6] delimited the functional nucleotide polymorphisms for *qSW5* within a 2,263-bp fragment of the Kasalath genomic region (FMR2, Supplementary Fig. 1). Compared with the corresponding region of Kasalath, the Nipponbare region harbours a 1,212-bp deletion and several single nucleotide polymorphisms. Thus, it was deduced that the 1,212-bp deletion represents the functional nucleotide polymorphism for *qSW5* (ref. 6). To verify this notion, we measured the grain width and sequenced a 6.3-kb upstream region of *GW5* in 19 wild rice accessions (*Oryza rufipogon*), 71 landraces and 39 breeding cultivars (the 110 cultivars including 54 *indica* and 56 *japonica* races), collected from diverse geographical locations across Asia (Supplementary Table 1). We uncovered 417 polymorphic sites and performed association studies (Supplementary Table 2), which confirmed significant association between the 1,212-bp deletion and grain width ($P = 4.83 \times 10^{-5}$) (Fig. 2d). Sequence analysis also revealed that only one wild rice harbours

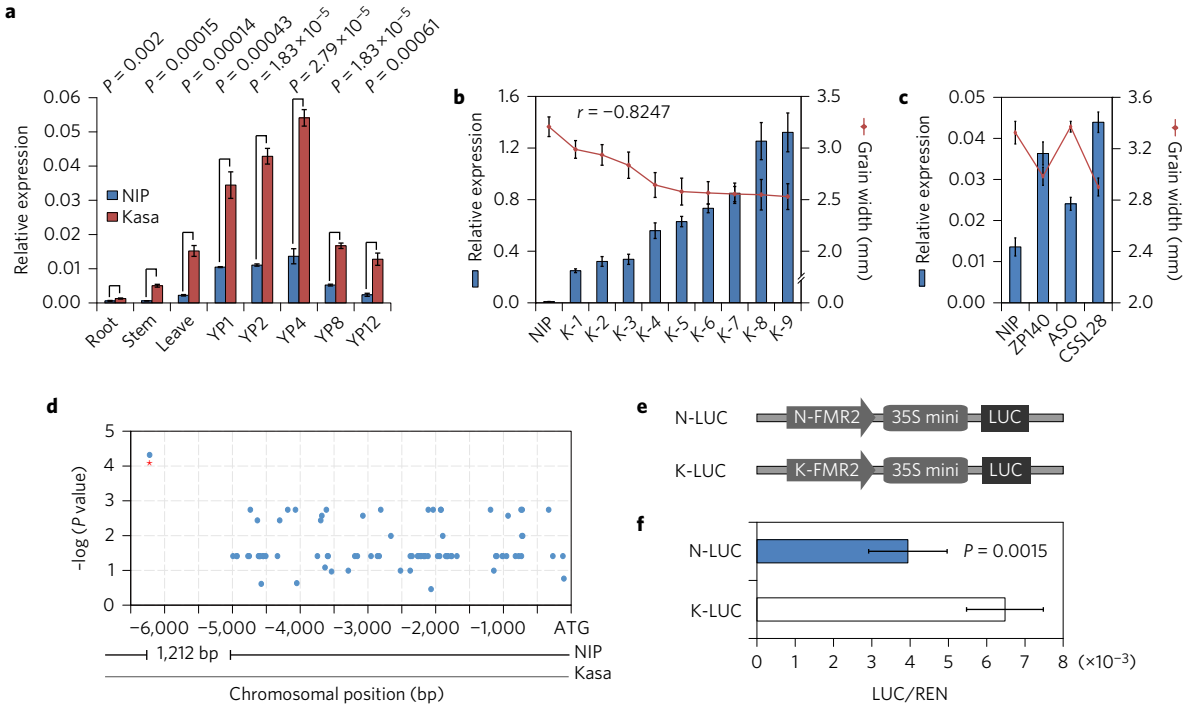

Figure 2 | The 1,212-bp deletion affects grain width through influencing *GW5* expression. a, RT-qPCR analysis of *GW5* expression in various organs of Nipponbare (NIP) and Kasalath (Kasa) plants, including root, stem, leaf and young panicle of 1 cm (YP1) to 12 cm (YP12) in length ($n = 3$). *P* values from the student's *t*-test are indicated. **b**, Negative correlation of grain width and the *GW5* expression level of transgenic plants (T1 families, *K-1* to *K-9*). Young panicles (~5 cm in length) were used. **c**, Transcript levels of *GW5* in Nipponbare and ZP140 (a near isogenic line with substitution of Kasalath chromosome 5 fragment in the Nipponbare background), Asominori (ASO) and CSSL28 (a near isogenic line with substitution of IR24 chromosome 5 fragment in the Asominori background) ($n = 3$). Young panicles (~5 cm in length) were used. Grain width is shown by the red line. **d**, Association study shows that the 1,212-bp deletion (indicated by the red asterisk), located ~5 kb upstream of the start codon of *GW5*, is associated with grain width. Blue dots indicate the significant levels of polymorphic sites associated with the grain width trait. **e**, Schematic representation of the N-LUC and K-LUC constructs for the reporter gene assay. N-FMR2, the fine mapping region of Nipponbare; K-FMR2, the fine mapping region of Kasalath; 35S mini, the 35S minimal promoter (−90). **f**, Luciferase reporter assay ($n = 6$ independent repeats). *P* values from the student's *t*-test are indicated. The values in **a**–**c** and **f** represent the mean ± s.d.

the 1,212-bp deletion, whereas all other accessions with the 1,212-bp deletion belong to the *japonica* group (Supplementary Fig. 15). Moreover, the average silent nucleotide variation across this 6.3-kb region was lower in landrace-*japonica* ($\pi sil = 0.00097$; $\theta sil = 0.00177$) than in *O. rufipogon* ($\pi sil = 0.01547$; $\theta sil = 0.01992$) and landrace-*indica* ($\pi sil = 0.00640$; $\theta sil = 0.00707$). Tajima's *D* test in the *japonica* population (Tajima's $D = -1.71117$, $0.05 < P < 0.1$) also confirmed the departure of a rare allele from neutrality. In addition, this region was further selected in breeding-*japonica* ($\pi sil = 0.00069$; $\theta sil = 0.00174$; Tajima's $D = -2.35624$, $P < 0.01$). We next performed Hudson–Kreitman–Aguade tests[10] across unlinked or loosely linked loci to discriminate the effects of selection forces versus population demography on this region during the speciation process. Hudson–Kreitman–Aguade tests with a set of known neutral genes (*Adh1, GBSSII, Ks1, Lhs1, Os0053, SSII1* and *TFIIAγ-1*)[11] as controls showed that the diversity of this region is significantly deviated from the neutral genes ($X^2 = 20.16$, $P = 0.022$ for landraces; $X^2 = 18.86$, $P = 0.039$ for breeding varieties). Further, a transient expression assay of a luciferase reporter gene driven by the upstream fine mapping region (FMR2, Supplementary Fig. 1) of Kasalath (K-FMR2) and Nipponbare (N-FMR2) fused to the 35S minimum promoter (−90) showed that K-FMR2 more effectively enhanced the expression of the reporter gene than N-FMR2 (Fig. 2e,f). Together, these results suggest that the 1,212-bp deletion was selected during *japonica* domestication and breeding for its effect on increased grain yield, most likely through influencing *GW5* expression. Similarly, previous studies have reported that natural variations in the regulatory region could regulate important agronomic traits through affecting downstream gene expression[12,13].

Next, we used the carboxyl-terminal region of Kasalath GW5 (GW5-C1, aa: 251–469) as the bait to screen a prey library constructed with mRNAs derived from the young panicle of Nipponbare. GSK2 (LOC_Os05g11730), a rice orthologue of *Arabidopsis* GSK3/SHAGGY-like kinase BIN2, was identified as a GW5-interacting partner. In addition, GW5-C2 (aa: 109–469) and GW5-C3 (aa: 319–469) also interacted with GSK2 (Fig. 3a,b). The interaction between GW5 and GSK2 was also confirmed by the split ubiquitin-based yeast two-hybrid assay (Supplementary Fig. 16), bimolecular fluorescence complementation (BiFC) assay (Fig. 3c) and *in vitro* pull-down assay (Fig. 3d).

It was previously reported that *GSK2* acts as a negative regulator of brassinosteroid (BR) signalling in rice. The *GSK2*-overexpressing plants (*Go*) had small round grains whereas the *GSK2* RNAi transgenic plants (*Gi*) displayed a slender and longer grain phenotype, compared with wild type[14]. We noted that in addition to slender seeds, the *GW5* overexpressors (*OX3*) displayed a typical enhanced BR-responsive phenotype, characterized as longer and narrower leaves with greatly increased leaf angles, resembling the phenotype of the transgenic plants overexpressing *DLT*[14,15]. Although to a lesser degree, the *J17* and *J20* transformants also displayed a minor BR-responsive phenotype (Supplementary Fig. 17). Lamina inclination experiments showed that *OX3* were hypersensitive to exogenously applied brassinolides (BLs) compared to the wild-type plants (Supplementary Fig. 18). These results suggest that *GW5* acts positively in the BR signalling pathway. Notably, overexpression of *GW5* in the *GSK2* overexpressing background (Go^{OX3}) produced grains more slender and longer than the *Go* plants, but wider and shorter than the *Gi* plants. In addition, overexpression

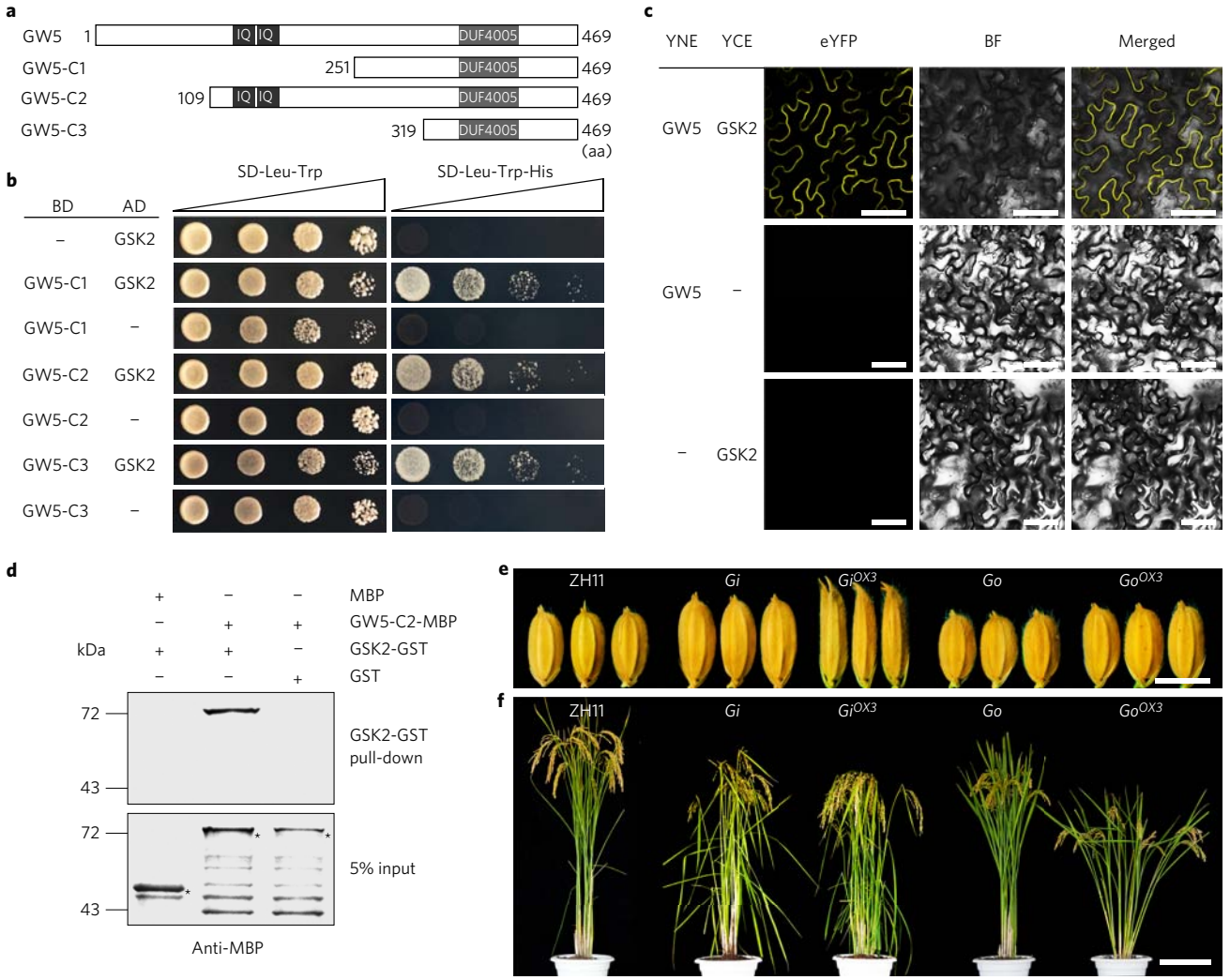

Figure 3 | GW5 physically interacts with GSK2 and is involved in BR signalling in rice. a, Schematic representation of the different truncated versions of GW5. **b**, GAL4-based Y2H assay shows that GSK2 interacts with GW5-C1, GW5-C2 and GW5-C3. AD, activation domain; BD, binding domain; SD, synthetic dropout; the gradients indicate tenfold serial dilutions. **c**, BiFC analysis of GW5 and GSK2 interaction. BF, bright field. Scale bars, 50 μm. **d**, GST pull-down assay showing the interaction between GW5-C2-MBP and GSK2-GST. Asterisks stand for the band of MBP or GW5C2-MBP. **e**, Seed morphology of wild type (Zhonghua 11, ZH11), *Gi, Go, Gi*^{OX3}and *Go*^{OX3}. Scale bar, 5 mm. **f**, Gross morphology of wild type (ZH11), *Gi, Go, Gi*^{OX3} and *Go*^{OX3} at the grain-filling stage. Scale bar, 20 cm.

of *GW5* in *Gi* background (*Gi*^{OX3}) resulted in greatly enlarged lamina bending and more slender grains compared with either the *Gi* or wild-type plants (Fig. 3e,f and Supplementary Fig. 19). These results suggest that *GW5* likely acts upstream of *GSK2* in the control of grain size and lamina bending.

Previous studies reported that GSK2 can phosphorylate OsBZR1 and DLT and inhibit their activities[14]. To test the possible regulatory effects of GW5 on GSK2, we conducted an *in vitro* kinase assay. We found that GSK2-GST could phosphorylate itself and its autophosphorylation activity was significantly repressed by GW5-C2-GST. Notably, we also observed weak phosphorylation of GW5-C2-GST by GSK2-GST (Fig. 4a). Further, when OsBZR1-MBP and DLT-MBP were used as the substrates for the assay, their phosphorylation by GSK2 was gradually inhibited by increasing amounts of GW5-C2-GST (Fig. 4b,c). A smaller truncated fusion protein, GW5-C3-MBP (GW5-C3 fused to MBP), also could repress the kinase activity of GSK2, suggesting that the C-terminal region of GW5 is responsible for its repressive activity on GSK2 (Fig. 3a and Supplementary Fig. 20a,b). Interestingly, mutations in the IQ motifs (GW5m-C2-GST) rendered a reduced repressive effect on GSK2 kinase activity (Supplementary Fig. 20c,d), suggesting that the IQ motifs of GW5 play a regulatory role in repressing the kinase activity of GSK2

As phosphorylated OsBZR1 is subject to 26S proteasome-mediated degradation[16], we next examined the effects of *GW5* overexpression on the levels and forms of GSK2, OsBZR1 and DLT proteins in *OX3* plants. Immunoblot with anti-GSK2, anti-OsBZR1 and anti-DLT antibodies detected two distinct bands with total rice extracts but the slower migrating band disappeared or became weaker when the total protein samples were treated with calf intestine alkaline phosphatase (CIP), indicating that the slower migrating bands represent phosphorylated forms of GSK2, OsBZR1 and DLT. Also, we found that *OX3* accumulated more dephosphorylated GSK2, OsBZR1 and DLT and less phosphorylated GSK2, OsBZR1 and DLT compared with Nipponbare (Fig. 4d–f and Supplementary Fig. 21a). Similar observations were made in the *J20* transformant (Supplementary Fig. 21b,c). These results support the notion that GW5 can repress both autophosphorylation of GSK2 and trans-phosphorylation of OsBZR1 and DLT by GSK2 *in vivo*, thus promoting the accumulation of unphosphorylated OsBZR1 and DLT proteins in the nucleus to mediate downstream BR responses. In support of this notion, RT–qPCR analysis revealed

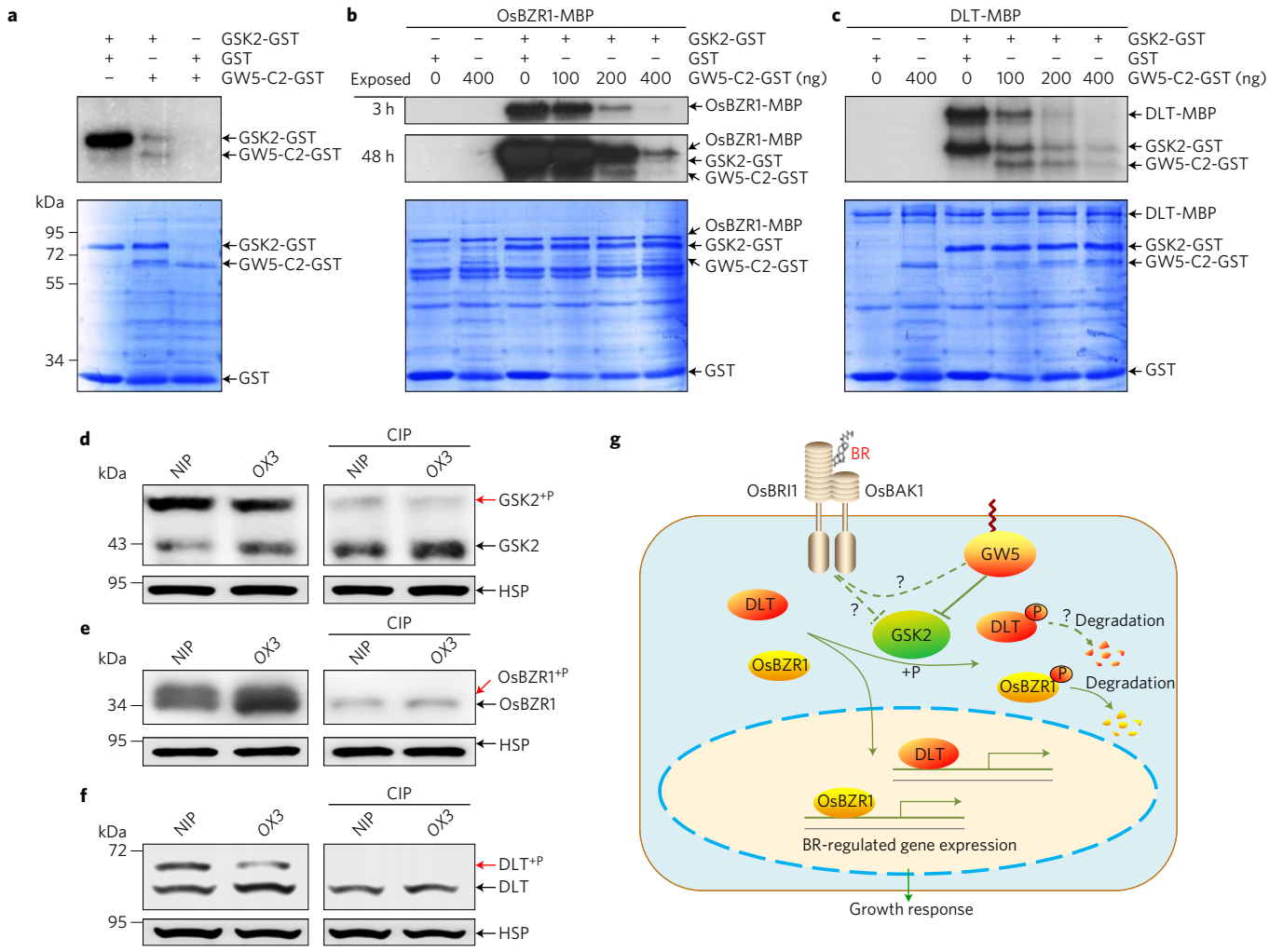

Figure 4 | GW5 represses GSK2 kinase activity on OsBZR1 and DLT. a–c, *In vitro* phosphorylation assay. The autophosphorylation of GSK2-GST (**a**), trans-phosphorylation of OsBZR1-MBP (**b**) and DLT-MBP (**c**) by GSK2-GST can be repressed by GW5-C2-GST. The corresponding lower panels show Coomassie blue staining of the proteins used for the phosphorylation assay. 3 h and 48 h indicate the exposure time. **d–f**, Immunoblot analysis of GSK2 (**d**), OsBZR1 (**e**) and DLT (**f**) proteins in *OX3* plants compared with Nipponbare (NIP). Black triangle indicates the phosphorylated band of OsBZR1 (**e**). Leaves of 2-month-old seedlings were used for **d** and **e**, ~12 cm length young panicles were used for **f**. Anti-HSP82 was used as a loading control. **g**, A proposed working model for *GW5*. BR and GW5 induce accumulation of unphosphorylated OsBZR1 and DLT proteins in the nucleus by repressing GSK2 kinase activity towards OsBZR1 and DLT, thus activating BR-regulated gene expression and growth response. The question marks indicate areas awaiting further investigation.

that three representative BR biosynthetic genes (*D2, DWARF* and *CPD*) were downregulated, whereas the BR-responsive gene *BU1* was upregulated in *OX3* and *Gi* plants (Supplementary Fig. 22).

Recent studies have shown that in analogy to the well-characterized BR signalling pathway in *Arabidopsis*[3], BR binding to OsBRI1 promotes its association with OsBAK1 (*Oryza sativa* BRI1 ASSOCIATED RECEPTOR KINASE1) and inactivates GSK2 in rice. GSK2 phosphorylates OsBZR1, LIC and DLT and inhibits their activity by promoting proteasome-mediated degradation of these factors[3,14]. Furthermore, it was recently shown that GSK2 can directly interact with OsGRF4 and inhibit its transcriptional activation activity to mediate the regulation of grain size[17–19]. However, the mechanism of GSK2 inhibition by activated OsBRI1 (*Oryza sativa* BRASSINOSTEROID INSENSITIVE1) and OsBAK1 remains unknown, as orthologous components of Arabidopsis BR signalling involved in BIN2 inactivation, such as BSKs and BSU1, have not been identified in rice up to now[5]. In this work, we identified a novel signalling component of the BR signalling pathway in rice. Our results suggest that *GW5*, which encodes a novel calmodulin-binding protein, acts positively and upstream of *GSK2* in the BR signalling pathway in rice. We provide evidence that GW5 can physically interact with GSK2 and inhibits its kinase activity towards OsBZR1 and DLT, leading to accumulation of unphosphorylated OsBZR1 and DLT proteins in the nucleus, and ultimately influences BR-responsive gene expression, grain size and weight in rice (Fig. 4g). The cloning of *GW5* marks an important step towards elucidating the molecular mechanisms controlling seed/grain size in cereal crops and the BR signalling network in higher plants. Moreover, knocking out *GW5* in Kasalath significantly increased its grain width and weight. Thus, *GW5* could serve as a viable candidate gene for targeted genome editing to improve grain yield in the future.

Methods

Plant materials and trait measurement. Nipponbare was used for the transgenic experiments unless indicated otherwise. For each construct, more than 20 independent transgene-positive lines (T0) were generated, and representative T1 plants displaying the typical phenotype were randomly chosen for trait measurement. Fully filled grains were used to measure 1,000-grain weight, and 30 grains were measured by an electronic digital-display Vernier calliper to obtain grain length and width. Rice plants were grown in a paddy field in Beijing, China.

RNA extraction, RACE and RT–qPCR. Total RNA was extracted using the RNeasy Plant Mini Kit (QIAGEN). cDNA was synthesized using the QuantiTect Reverse Transcription Kit (QIAGEN). For the RACE assay, the full-length transcripts of

ORF3 were amplified by nested PCR with the SMARTer RACE cDNA Amplification kit (Clontech). RT–qPCR was carried out using the Ex Taq Kit (TaKaRa) in an ABI PRISM 7900HT (Applied Biosystems) according to the manufacturer's instructions. The rice ubiquitin gene (LOC_Os03g13170) was used as the internal control. Three biological repeats were performed for each gene, and the average values and standard deviations are shown. The gene-specific primers used for RT–qPCR are listed in Supplementary Table 3.

Construct generation and transformation. To generate *OX1*, *OX2* and *OX3* constructs, the full-length ORF1, ORF2 and ORF3 were amplified from the cDNA of Kasalath plants and then cloned into the binary vector pCAMBIA1390, respectively. For the complementation test, different genomic fragments were amplified from the Kasalath genomic DNA and cloned into the binary vector pCAMBIA1305. To generate the *K-OX* and *N-OX* constructs, the CaMV 35S enhancer fragment (−421 to −92) region[25,26] was amplified and fused to the promoter region of *GW5* from Kasalath, then fused to the CDS region of Kasalath and Nipponbare, respectively. To generate the *OX3m* construct, the mutated sequences (aAVRiqTAfrGFLAkkALRALKaLVKlq to replace DAVRTHTAVTGFLANTALRALKELVKQK) of ORF3 cDNA (aa: 136–163) were cloned into pCAMBIA1390. For the CRISPR test, the oligonucleotides used for targeted mutagenesis were designed online and then cloned into a CRISPR–Cas9 plant expression vector[20]. To generate the *pUBI::GW5-GFP* constructs, full-length cDNA of *GW5* was cloned into the binary vector AHLG. To create the *pGW5::GUS* construct, a 2.56-kb promoter fragment from Kasalath was cloned into the binary vector pCAMBIA1305. Relevant primers are listed in Supplementary Table 3. All the resulting binary plasmids were transformed into the *Agrobacterium tumefaciens* strain *EHA105* and used to transform rice calli. All constructs were sequencing-verified.

Fluorescence microscopy observation and GUS (β-glucuronidase) staining. The transformed rice protoplasts, infiltrated tobacco leaves, onion epidermal cells and transgenic rice roots were sampled for GFP or YFP fluorescence observation. GFP and YFP were observed under a confocal fluorescence microscope (Leica TCS SP6). GUS staining was performed as previously described[21].

Association study and sequence analysis. The association analyses were performed using the TASSEL software (version 3.0). Only polymorphic markers present at an allele frequency >5% were included to detect associations by using the MLM (mixed linear model) in TASSEL[22]. The average number of nucleotide diversity at silent sites (π_{sil}) was calculated using DNASP version 5 (ref. 23). The neutral evolution of population was tested by Tajima's *D* test[24].

Yeast two-hybrid assays. The cDNA of GSK2 was cloned into the Y2H 'prey' vector, pGADT7 (Clontech). Three C-terminal fragments of GW5 (GW5-C1, aa 251–469; GW5-C2, aa 109–469; GW5-C3, aa 319–469) cDNA were cloned into the Y2H 'bait' vector pGBKT7 (Clontech), respectively, and used for GAL4-based yeast two-hybrid screen and interaction studies. Bait and prey constructs were co-transformed into the yeast strain AH109. For split ubiquitin-based yeast two-hybrid assay, the cDNA of *GSK2* was fused to the NubG fragment in the pPR3-N vector. The full-length cDNA of *GW5* was fused to the Cub-LexA-VP16 fragment in the pDHB1 vector. Interaction was determined by co-transformation of the prey and bait vectors into the yeast strain NMY51, supplied by the DUAL hunter system according to the manufacturer's instructions. Co-transformed yeast clones were serially diluted (1:10) and then spotted on the control medium and selective medium for growth.

BiFC and luciferase reporter assays. For BiFC analysis, cDNA of *GSK2* was cloned into the pSPYCE(M) (eYCE) vector, whereas cDNA of *GW5* was cloned into the pSPYNE(M) (eYNE) vector, respectively. For luciferase reporter assays, the genomic fragments corresponding to the 2,263-bp fine mapping region were amplified from Kasalath and Nipponbare, respectively, then fused to the 35S minimal promoter (-90) and cloned into pGreen 0800-LUC vector, respectively. The plasmids were expressed in tobacco leaf epidermis cells by Agrobacterium-mediated infiltration. BiFC analysis was performed as described previously[25,26]. Luciferase activity was measured using the Dual-Luciferase reporter assay system (Promega, E1910).

***In vitro* pull-down assays.** The *in vitro* pull-down assay was performed as reported previously[27]. Five milligrams of GST- or GSK2-GST-coupled beads were used to pull down 5 mg MBP or GW5-C2-MBP protein. Anti-MBP antibodies (New England Biolabs) were used to detect the output protein.

***In vitro* phosphorylation assays.** Phosphorylation assays were performed with recombinant fusion proteins as reported previously[14,26]. GST (800 ng), GW5-C2-GST or GW5m-C2-GST (C2 fragment of GW5 or GW5m fused to GST, the mutated sequences of the GW5m is the same as ORF3m, 500 ng or marked in the figure), MBP (800 ng) or GW5-C3-MBP (C3 fragment of GW5 fused to MBP, 800 ng) together with GSK2-GST (800 ng) recombinant proteins were incubated at 30 °C for 2.5 h with BZR1-MBP (300 ng) or DLT-MBP (600 ng) recombinant proteins, respectively. The reaction was then terminated and separated on a 10% SDS–PAGE gel. The gel was stained with Coomassie blue and imaged, then exposed to GE Amersham hyperfilm MP film for 3–48 h to detect phosphorylation.

Immunoblot detection of GSK2, DLT and OsBZR1 proteins in plants. Commercial anti-GSK2, anti-BZR1, anti-DLT and anti-HSP polyclonal antibodies were purchased from BPI (http://www.proteomics.org.cn) and used to detect GSK2, BZR1, DLT and HSP, respectively. Total protein was isolated from the *OX3* plants, *J20* plants and Nipponbare. For OsBZR1, plant materials were ground into fine powder in liquid nitrogen and the samples were directly boiled with 1 × SDS sample buffer (5 μl per mg) at 95 °C for 15 min, then centrifuged. The supernatants were used for SDS–PAGE and immunoblot analysis. For GSK2 and DLT, total proteins were extracted in an RIPA buffer[26] and then denatured in SDS sample buffer. For CIP treatment, the extracts were incubated with CIP at 37 °C for 25 min. Anti-DLT, anti-GSK2, anti-OsBZR1 and anti-HSP antibodies were used with dilutions of 1:1000, 1:500, 1:500 and 1:10,000, respectively. Immunoblot analysis was performed as previously reported[14].

BL induction analysis. The lamina joint bending assay using excised leaf segments was performed as reported previously[28]. BL was purchased from Sigma (http://www.sigmaaldrich.com/). Lamina joint angles were measured using the ImageJ software.

Phylogenetic analysis of the GW5-like proteins in higher plants. Phylogenetic analysis was conducted using MEGA 5. The sequences of 14 GW5 homologues were obtained from NCBI (http://www.ncbi.nlm.nih.gov/) and used to establish a bootstrap neighbour-joining phylogenetic tree. One-thousand replicates were conducted to determine the statistical support for each node.

Data availability. All relevant data are available upon request from the corresponding authors. The sequence of the *GW5* coding region has been deposited in the GenBank database under the accession numbers KT895078 (Nipponbare) and KT895079 (Kasalath), respectively.

Received 23 February 2016; accepted 7 March 2017; published 10 April 2017

References

1. Sweeney, M. & McCouch, S. The complex history of the domestication of rice. *Ann. Bot.* **100,** 951–957 (2007).
2. Zuo, J. & Li, J. Molecular genetic dissection of quantitative trait loci regulating rice grain size. *Annu. Rev. Genet.* **48,** 99–118 (2014).
3. Zhang, C., Bai, M. Y. & Chong, K. Brassinosteroid-mediated regulation of agronomic traits in rice. *Plant Cell Rep.* **33,** 683–696 (2014).
4. Hu, X. *et al.* The U-box E3 ubiquitin ligase TUD1 functions with a heterotrimeric G α subunit to regulate brassinosteroid-mediated growth in rice. *PLoS Genet.* **9,** e1003391 (2013).
5. Weng, J. *et al.* Isolation and initial characterization of *GW5*, a major QTL associated with rice grain width and weight. *Cell Res.* **18,** 1199–1209 (2008).
6. Shomura, A. *et al.* Deletion in a gene associated with grain size increased yields during rice domestication. *Nat. Genet.* **40,** 1023–1028 (2008).
7. Wang, X. *et al. Trans*-golgi network-located AP1 gamma adaptins mediate dileucine motif-directed vacuolar targeting in *Arabidopsis*. *Plant Cell* **26,** 4102–4118 (2014).
8. Chen, X., Huang, H. & Xu, L. The CaMV 35S enhancer has a function to change the histone modification state at insertion loci in *Arabidopsis thaliana*. *J. Plant Res.* **126,** 841–846 (2013).
9. Benfey, P. N., Ren, L. & Chua, N. H. The CaMV 35S enhancer contains at least two domains which can confer different developmental and tissue-specific expression patterns. *EMBO J.* **8,** 2195–2202 (1989).
10. Hudson, R. R., Kreitman, M. & Aguadé, M. A test of neutral molecular evolution based on nucleotide data. *Genetics* **116,** 153–159 (1987).
11. Zhu, Q., Zheng, X., Luo, J., Gaut, B. S. & Ge, S. Multilocus analysis of nucleotide variation of *Oryza sativa* and its wild relatives: severe bottleneck during domestication of rice. *Mol. Biol. Evol.* **24,** 875–888 (2007).
12. Liu, L. *et al. KRN4* controls quantitative variation in maize kernel row number. *PLoS Genet.* **11,** e1005670 (2015).
13. Ishii, T. *et al. OsLG1* regulates a closed panicle trait in domesticated rice. *Nat. Genet.* **45,** 462–465 (2013).
14. Tong, H. *et al.* DWARF AND LOW-TILLERING acts as a direct downstream target of a GSK3/SHAGGY-like kinase to mediate brassinosteroid responses in rice. *Plant Cell* **24,** 2562–2577 (2012).
15. Sun, S. *et al.* Brassinosteroid signaling regulates leaf erectness in *Oryza sativa* via the control of a specific U-type cyclin and cell proliferation. *Dev. Cell* **34,** 220–228 (2015).
16. He, J. X., Gendron, J. M., Yang, Y., Li, J. & Wang, Z. Y. The GSK3-like kinase BIN2 phosphorylates and destabilizes BZR1, a positive regulator of the brassinosteroid signaling pathway in *Arabidopsis*. *Proc. Natl Acad. Sci. USA* **99,** 10185–10190 (2002).
17. Duan, P. *et al.* Regulation of *OsGRF4* by *OsmiR396* controls grain size and yield in rice. *Nat. Plants* **2,** 15203 (2015).
18. Hu, J. *et al.* A rare allele of *GS2* enhances grain size and grain yield in rice. *Mol. Plant* **8,** 1455–1465 (2015).

19. Che, R. *et al.* Control of grain size and rice yield by *GL2*-mediated brassinosteroid responses. *Nat. Plants* **2,** 15195 (2015).
20. Lei, Y. *et al.* CRISPR-P: a web tool for synthetic single-guide RNA design of CRISPR-system in plants. *Mol. Plant* **7,** 1494–1496 (2014).
21. Jefferson, R. The GUS reporter gene system. *Nature* **342,** 837–838 (1989).
22. Bradbury, P. J. *et al.* TASSEL: software for association mapping of complex traits in diverse samples. *Bioinformatics* **23,** 2633–2635 (2007).
23. Rozas, J., Sanchez-DelBarrio, J. C., Messeguer, X. & Rozas, R. DnaSP, DNA polymorphism analyses by the coalescent and other methods. *Bioinformatics* **19,** 2496–2497 (2003).
24. Tajima, F. Statistical method for testing the neutral mutation hypothesis by DNA polymorphism. *Genetics* **123,** 585–595 (1989).
25. Waadt, R. & Kudla, J. In planta visualization of protein interactions using bimolecular fluorescence complementation (BiFC). *CSH Protoc.* http://dx.doi.org/10.1101/pdb.prot4995 (2008).
26. Lin, Q. *et al.* The SnRK2-APC/CTE regulatory module mediates the antagonistic action of gibberellic acid and abscisic acid pathways. *Nat. Commun.* **6,** 7981 (2015).
27. Miernyk, J. A. & Thelen, J. J. Biochemical approaches for discovering protein–protein interactions. *Plant J.* **53,** 597–609 (2008).
28. Wada, K., Marumo, S., Ikekawa, N., Morisaki, M. & Mori, K. Brassinolide and homobrassinolide promotion of lamina inclination of rice seedlings. *Plant Cell Physiol.* **22,** 323–325 (1981).

Acknowledgements

We thank C. Chu (Chinese Academy of Sciences) for kindly providing the Go and Gi transgenic seeds; we thank X.W. Deng (Peking University), C. Wu (Chinese Academy of Agricultural Sciences) and J. Zhou (Frontier Laboratories of Systems Crop Design) for technical support. This work was supported by the National Natural Science Foundation of China (No. 91535302 and No. 31430008), National Key Research and Development Plan (2016YFD0100400) and National Transformation Science and Technology Program (2014ZX08001006).

Author contributions

J.L. and J.C. performed most of the experiments; X.Zheng performed the analysis of molecular evolution; F.W., Q.L, Y.H., P.T., Z.C. and X.Y. provided technical assistance; K.Z. performed some of the sub-cellular localization assay; X.Zhang and X.G. generated the transgenic plants; J.Wang cultivated the transgenic plants in the field; J.Wan and H.W. supervised the project; J.Wan, H.W. and J.L. designed the research and wrote the manuscript.

Additional information

Supplementary information is available for this paper.

Reprints and permissions information is available at www.nature.com/reprints.

Correspondence and requests for materials should be addressed to H.W. and J.W.

How to cite this article: Liu, J. *et al. GW5* acts in the brassinosteroid signalling pathway to regulate grain width and weight in rice. *Nat. Plants* **3,** 17043 (2017).

Publisher's note: Springer Nature remains neutral with regard to jurisdictional claims in published maps and institutional affiliations.

Competing interests

The authors declare no competing financial interests.